



Original article

Oxidation resistance 1 regulates post-translational modifications of peroxiredoxin 2 in the cerebellum

Daria M. Svistunova^a, Jillian N. Simon^b, Elzbieta Rembeza^c, Mark Crabtree^b, Wyatt W. Yue^c, Peter L. Oliver^{a,d,*}, Mattéa J. Finelli^{a,*}^a Department of Physiology, Anatomy and Genetics, University of Oxford, Oxford OX1 3PT, UK^b Division of Cardiovascular Medicine, Radcliffe Department of Medicine, John Radcliffe Hospital, University of Oxford, Oxford OX3 9DU, UK^c Structural Genomics Consortium, Nuffield Department of Clinical Medicine, University of Oxford, OX3 7DQ, UK^d MRC Harwell Institute, Harwell Campus, Oxfordshire OX11 0RD, UK

ARTICLE INFO

Keywords:

Oxidative stress
Chaperone
Antioxidant
Peroxiredoxin
Neurodegeneration
Mouse

ABSTRACT

Protein aggregation, oxidative and nitrosative stress are etiological factors common to all major neurodegenerative disorders. Therefore, identifying proteins that function at the crossroads of these essential pathways may provide novel targets for therapy. Oxidation resistance 1 (Oxr1) is a protein proven to be neuroprotective against oxidative stress, although the molecular mechanisms involved remain unclear. Here, we demonstrate that Oxr1 interacts with the multifunctional protein, peroxiredoxin 2 (Prdx2), a potent antioxidant enzyme highly expressed in the brain that can also act as a molecular chaperone. Using a combination of *in vitro* assays and two animal models, we discovered that expression levels of Oxr1 regulate the degree of oligomerization of Prdx2 and also its post-translational modifications (PTMs), specifically suggesting that Oxr1 acts as a functional switch between the antioxidant and chaperone functions of Prdx2. Furthermore, we showed in the Oxr1 knockout mouse that Prdx2 is aberrantly modified by overoxidation and S-nitrosylation in the cerebellum at the pre-symptomatic stage; this in-turn affected the oligomerization of Prdx2, potentially impeding its normal functions and contributing to the specific cerebellar neurodegeneration in this mouse model.

1. Introduction

Neurodegenerative disorders are becoming more prevalent with increased global life expectancy and a better understanding of the underlying disease mechanisms will be essential for designing new therapeutic approaches to tackle this growing health burden [1–3]. Aberrant proteostasis and increased oxidative and nitrosative (O/N) stress have been strongly linked with the neurodegenerative process, irrespective of the etiology [4,5]. O/N stress arises from an excessive accumulation of reactive oxygen species (ROS) and reactive nitrogen species (RNS) resulting from an imbalance between free radical production and detoxification by antioxidant proteins [6]. Elevated levels of O/N stress markers such as oxidised lipids and nitrated proteins have

been reported in *post mortem* tissue of individuals affected by major neurodegenerative disorders such as Alzheimer's disease (AD), Parkinson's disease (PD), and amyotrophic lateral sclerosis (ALS) [7–9]. Importantly, these markers are not only observed at the end-stage of the disease but are also detected in peripheral blood of patients during the course of the disease and pre-symptomatically in animal models of these conditions [10–14]. For example, mouse models of ALS show elevated levels of carbonylated proteins, a marker of ROS-induced protein damage, before any motor neuron pathology or clinical features are observed, suggesting that O/N stress is an early event of the neurodegenerative process [15].

Protein aggregation is another important feature consistently observed in neurodegenerative disease. Indeed, the formation of

Abbreviations: Oxr1, Oxidation resistance 1; Prdx2, peroxiredoxin 2; PTMs, post-translational modifications; O/N, oxidative and nitrosative; ROS, reactive oxygen species; RNS, reactive nitrogen species; AD, Alzheimer's disease; PD, Parkinson's disease; ALS, amyotrophic lateral sclerosis; PDI, protein disulfide-isomerase; TBC1D24, TBC1 Domain Family Member 24; DOORS, deafness, onychodystrophy, osteodystrophy and mental retardation with seizures; Ncoa7, nuclear receptor coactivator 7; HMW, high molecular weight; GPI/Gpi1, glucose-6-phosphate isomerase; Oxr1-FL, full-length Oxr1; CS, citrate synthase; SNO-C, S-nitrosocysteine; SNO-protein, S-nitrosylated protein; ORC, organomercury resin capture; BCA, bicinchoninic acid; IPTG, isopropyl β-D-1-thiogalactopyranoside; FOX, ferrous oxidation-xylenol orange; veh, vehicle; DTT, dithiothreitol

* Corresponding authors. Department of Physiology, Anatomy and Genetics, University of Oxford, Oxford OX1 3PT, UK.

E-mail addresses: p.oliver@har.mrc.ac.uk (P.L. Oliver), mattea.finelli@ndcn.ox.ac.uk (M.J. Finelli).

<https://doi.org/10.1016/j.freeradbiomed.2018.10.447>

Received 24 July 2018; Received in revised form 28 October 2018; Accepted 29 October 2018

Available online 31 October 2018

0891-5849/ Crown Copyright © 2018 Published by Elsevier Inc. This is an open access article under the CC BY-NC-ND license (<http://creativecommons.org/licenses/by-nc-nd/4.0/>).

neurotoxic protein aggregates has been reported in brain and spinal cord regions affected by AD, PD, and ALS [16]. In normal conditions, chaperone proteins are employed to fold misfolded proteins and disassemble protein aggregates, and thus play a key role in the global cellular proteostasis [17]. In neurodegenerative disease, however, the chaperone activity in cells is disrupted. For instance, mutations in the gene encoding for the mitochondrial chaperone mtHsp70 have been identified in patients with PD, and have been shown to disrupt mtHsp70 activity and to lead to apoptosis [18,19]. In addition, PTMs, such as S-nitrosylation and sulfonylation, have been associated with dysregulation of protein function. For instance, aberrant S-nitrosylation of the chaperone protein disulfide-isomerase (PDI) inhibits its activity, leading to neurodegeneration [20,21]. Therefore, identifying proteins that function in both the O/N stress and proteostasis pathways may produce valuable insights into the underlying pathogenic mechanisms of neurodegenerative conditions.

Oxidation resistance 1 (OXR1) was originally identified as a gene capable of rescuing bacterial oxidative DNA damage [22]. Subsequently, Oxr1 has been shown to act as a potent regulator of oxidative stress in mammalian neurons that can also delay neurodegeneration *in vivo*. Oxr1 possesses a highly conserved C-terminal TLDc domain shared with four other proteins in mammals, several of which have been proven to be important for brain function [23]. Mutations in the TLDc domain of TBC1 domain family member 24 (TBC1D24) influence its role in neuronal cell development and function and are associated with a range of familial neurological disorders, including epilepsy and deafness, onychodystrophy, osteodystrophy and mental retardation with seizures (DOORS) syndrome [23–25]. Moreover, mice lacking all Oxr1 isoforms present a progressive ataxic phenotype concomitant with degeneration of granule neurons in the cerebellum from postnatal day 19 (P19) [26–28]. Conversely, over-expression of Oxr1 *in vivo* is able to delay motor neuron degeneration and motor dysfunction in a mouse model of ALS [29]. *In vitro* studies in mammalian cells also demonstrated that levels of Oxr1 can modulate the sensitivity of neurons to oxidative stress [26,28]: knock-down of Oxr1 leads to oxidative stress-induced cell death while over-expression of Oxr1 reduces ROS levels and apoptosis of cells subjected to oxidative stress [26,28]. Furthermore, studies in a range of experimental systems have demonstrated a dysregulation of the expression of a number of antioxidant genes when Oxr1 is disrupted. For example, glutathione peroxidase 2 (GPX2), heme oxygenase-1 (HO-1), catalase (CAT) and peroxiredoxin 4 are reportedly down-regulated in OXR1-depleted mammalian cell lines [30–32], whereas in mosquitos, gene knock-down of OXR1 regulates the basal levels of CAT and Gpx expression [33].

As well as Oxr1, the TLDc-containing protein nuclear receptor coactivator 7 (NcoA7) can reduce the levels of the O/N stress-induced PTM, S-nitrosylation, in neurons [26]; thus taken together, these data suggest that the TLDc proteins have the ability to reduce O/N stress. However, no superoxide dismutase or catalase-like catalytic activity has been detected for Oxr1, and the three-dimensional structure of the TLDc domain provides no clues regarding the molecular function of this important group of proteins [28,34,35]. In addition, Oxr1 has been shown to reduce the aggregation and mislocalisation of the ALS-associated proteins FUS and TDP-43 via protein interaction, although the precise mechanism involved is currently unclear [36].

Here, we demonstrate that Oxr1 interacts with peroxiredoxin 2 (Prdx2), a highly abundant and potent antioxidant enzyme that also possesses a chaperone function. Our results suggest that Oxr1 acts as a functional switch for Prdx2 activity, from an H₂O₂ scavenger to a high molecular weight (HMW) chaperone complex, through the modulation of its overoxidation and S-nitrosylation. We also report an unexpected and novel function for Oxr1 as a potential holdase.

2. Materials and methods

2.1. Reagents

Reagents used were as follows: Insulin (I0516, Sigma), citrate synthase (C3260, Sigma), protease inhibitor (5871S, Cell Signaling), protease/phosphatase inhibitor (5872S, Cell Signaling), protease inhibitor (11836170001, Roche). Antibodies used were: Prdx2 (10545–2-AP, Proteintech), Prdx-SO_{2/3} (ab16830, Abcam), β -actin (ab8226, Abcam), HA (H6908, Sigma), α -tubulin (Sigma), MYC (Sigma), Oxr1 [28].

2.2. Animals

Constitutive Oxr1 knockout (*Oxr1*^{d/d}) mice maintained on a C57BL6/J background have been previously described [27]. Oxr1 Tg mice, where a full-length cDNA transgene of Oxr1-FL is expressed from a ubiquitous actin-derived promoter, were also maintained on a C57BL6/J background and have been previously described [28]. All experiments were conducted in adherence with the guidelines set forth by the UK Home Office regulations, and with the approval of the University of Oxford Ethical Review Panel.

2.3. Expression constructs

Mouse Prdx2 cDNA (NM_001317385.1) was cloned from total brain cDNA extract into pET-22b vector with or without introducing thrombin cleavage site (Thr) in frame with a His₆ tag: F – 5'-GAGACA TATGGCCTCCGGCAACGCGCAAATC-3', R – 5'-GAGACTCGAGGCTGCC ACGCGGCACCAAGTTGTGTTTGGAGAAGTATTCC-3'; or F – 5'-GAGAC ATATGGCCTCCGGCAACGCGCAAATC-3', R – 5'-GAGACTCGAGGTTGT GTTTGGAGAAGTATTCC-3', respectively. Mouse Oxr1-C (NM_001130164) was cloned from total brain cDNA into pET-22b backbone in frame with His₆ tag (F – 5'-GAGACATATGTCCCGTCTCTG GTATGGGAAAAAAG-3', R – 5'-GAGACTCGAGTTCAAAAGCCAGATT TCAATG-3'). For expression in mammalian cells, mouse Prdx2 was cloned into pcDNA3.1 with a C-terminal MYC tag. All other constructs used have been previously described [26,28].

2.4. Cell culture, transfection, and treatment

Neuro2a (N2a) and SH-SY5Y cells were cultured in DMEM with GlutaMAX (Gibco) and Ham's F12:DMEM (Gibco) respectively, supplemented with 10% fetal bovine serum (Gibco) and 1% penicillin-streptomycin solution (Gibco) in an incubator at 37 °C in 5% CO₂ atmosphere. Cells were seeded 24 h prior to transfection. Cells were transfected using Fugene 6 (Promega) diluted in Opti-MEM (Gibco) according to manufacturer's protocol. 24 h after transfection culture media was changed to media supplemented with desired concentrations of H₂O₂. For cell death assay, cells were treated with 500 μ M H₂O₂ for 5 h, and for Prdx2 overoxidation experiments, cells were treated with 300 μ M H₂O₂ for 1 h. Fluorescent microscope Axioplan2 Imaging (Carl Zeiss) was used for cell death assay to visualise the pyknotic nuclei. For S-nitrosocysteine (SNOC) treatment of SH-SY5Y cells, a fresh stock solution of SNOC was prepared immediately before each use by mixing 200 mM cysteine (Sigma) with 200 mM NaNO₂ (Sigma) supplemented with HCl (0.5 N). Cells were treated with 200 μ M SNOC for 30 min. Control cells were treated with a vehicle solution (HCl diluted in water).

2.5. Immunoprecipitation and western blotting

SDS-PAGE- Tissue samples or cells were lysed in cold RIPA buffer supplemented with protease inhibitor (Cell signaling) and 1% Triton X-100 or 1% CHAPS in a tissue Precellys homogenizer (Bertin Corp.) (for tissue) or by trituration with a syringe (for cells). Protein concentration was assessed by bicinchoninic acid (BCA) assay (Novagen). For co-

immunoprecipitation, protein extracts were incubated overnight at 4 °C with either Prdx2 antibody, EZview MYC beads (Sigma) or G protein sepharose beads (Sigma) only, as a control. Protein-antibody complexes were pulled down using G protein sepharose beads (Sigma) and washed with cold RIPA buffer. Immunoprecipitated proteins were incubated with Laemmli loading buffer (Bio-Rad) or NuPAGE loading buffer (Life Technologies) supplemented with 5% β -mercaptoethanol (Sigma) at 100 °C for 5 min.

Blue Native-PAGE (BN-PAGE)- Brain and cerebella tissue samples and cells were homogenised in cold PBS buffer supplemented with protease/phosphatase inhibitors (New England Biolabs) using Precellys homogenizer (only for tissue samples) and lysed by repeated freezing and thawing (for tissue and cells). After measuring protein concentration using BCA assay (Novagen), samples were mixed with 5x loading buffer (62.5 mM Tris-HCl pH 6.8, 40% glycerol, 0.01% bromophenol blue) and were resolved on 10% Bis-Tris native gel.

After samples were run on either SDS-PAGE or BN-PAGE, proteins were transferred to PVDF membrane (Amersham). The membrane was then blocked with 5% skim milk in PBST for 1 h at room temperature and incubated overnight with primary antibodies at 4 °C. The membranes were washed with PBST and incubated with secondary HRP-conjugated antibodies and signal was detected using ECL or ECL Prime Western Blotting detection kit (both Amersham) using an ImageQuant LAS 4000 (GE Healthcare). Western blot signal was quantified using ImageJ.

2.6. Protein expression and purification

Prdx2-His₆ and Prdx2-Thr-His₆ proteins were produced in *E.coli* strain BL21(DE3) (Invitrogen) and purified according to protocol published by Yan et al. [37]. Briefly, protein expression was induced at OD₆₀₀ ~0.7–0.8 by addition of isopropyl β -D-1-thiogalactopyranoside (IPTG) (Sigma) to final concentration of 0.8 mM. After incubation on a shaker for 5 h at 25 °C, bacterial cells were collected by centrifugation and resuspended in 500 mM NaCl PBS supplemented with protease inhibitors. After sonication of the bacterial cultures and centrifugation for 30 min at 4 °C, recombinant His₆-tagged protein was incubated with 1 ml TALON metal affinity resin (Clontech) for 1 h at 4 °C. Proteins were washed using increasing concentration of imidazole, and eluted with 500 mM imidazole. Eluted samples were dialysed overnight against PBS buffer at 4 °C using Slide-A-Lyzer dialysis cassette (Thermo Fisher). The His₆ tag was cleaved from Prdx2-Thr-His₆ using the Thrombin Clean-Cleave Kit (Sigma Aldrich) at 17 °C for 4 h, as per the manufacturer's protocol and dialysed against PBS buffer following cleavage. Oxr1-C was produced as described before [28]. Briefly, protein expression was induced at OD₆₀₀ ~ 0.8 by addition of IPTG to a final concentration of 0.8 mM. Bacterial cultures were incubated on a shaker for 16 h at 18 °C and bacterial cells were collected by centrifugation. Protein was purified as described above. Full-length human OXR1 recombinant protein expressed in *E.Coli* was purchased from Origene (TP760961). Purified proteins were analysed by western blotting with anti-Prdx2 and anti-Oxr1 antibodies. Protein concentrations were measured using Nano-Drop spectrophotometer with extinction coefficients of 21,555 M⁻¹ cm⁻¹ for Prdx2 and 38,055 M⁻¹ cm⁻¹ for Oxr1-C and. DNA fragments encoding TB1D24 full-length (aa 1–553) and TLDc domain (aa 336–553) were subcloned into the pFB-Lic-Bse for insect Sf9 cell expression and pNIC28-Bsa4 for *E. coli* expression, respectively. Recombinant full-length TBC1D24 was expressed in Sf9 cells, while the TBC1D24 TLDc-domain was expressed in *E.Coli* and purified as above, followed by size exclusion chromatography. The purity of the recombinant protein preparation was ascertained by coomassie staining (Supplementary Fig. 1).

2.7. Peroxiredoxin activity assay

Prdx2 activity was assessed using ferrous oxidation-xylenol orange

(FOX) assay [38]. The assay solution contained 100 μ M dithiothreitol (DTT, Sigma Aldrich), 50 μ M H₂O₂ (Sigma Aldrich), 2.2 μ g recombinant uncleaved purified Prdx2, with 0 or 0.95 μ g Oxr1-C or 4.5 μ g OXR1-FL. The reaction was initiated by addition of H₂O₂ and quenched at appropriate time points by addition of 200 μ l of FOX reagent (1 part of FOX A reagent (25 mM ammonium ferrous sulfate (Sigma) in 2.5 M H₂SO₄ (Sigma)) and 100 parts of FOX B reagent (100 mM sorbitol (Sigma) with 125 μ M xylenol orange (Sigma) in water)). Samples were incubated at room temperature for at least 30 min before reading absorbance at 560 nm with Fluostar Omega plate reader.

2.8. Chaperone activity assay

In vitro holdase activity of cleaved Prdx2 and Oxr1-C was assessed in chemically- and thermally-induced aggregation assays. The ability of Prdx2 and Oxr1-C to protect insulin from DTT-induced aggregation was measured as change of absorbance at 650 nm at 25 °C. The reaction solution contained 30 μ g insulin (Sigma Aldrich) with or without 20 μ g Prdx2, with 22 μ g (6 μ M final concentration), 33 μ g (9 μ M) Oxr1-C, 22 μ g Tbc1d24, 22 μ g Tbc1d24 TLDc domain or 85 μ g (6 μ M) OXR1-FL and was initiated by addition of DTT to a final concentration of 6.66 mM. Ability of Prdx2 and Oxr1-C to protect citrate synthase (CS) from aggregating was monitored by changes in absorbance at 360 nm during incubation at 44 °C. Reaction solution contained 10 μ g of CS and 10 μ g of Prdx2, Oxr1-C or both in 50 mM HEPES pH 8.0.

2.9. Biotin switch assay

The biotin switch assay was performed as previously described using the reagents from the S-nitrosylated protein detection kit (Cayman) [39]. For tissue, snap-frozen brains or cerebella were homogenised in buffer A supplemented with protease inhibitors (Cell Signaling) using a tissue Precellys homogenizer (Bertin Corp.). After centrifugation at maximum speed for 30 min at 4 °C, protein concentration was quantified using a BCA assay (Thermo Scientific) and an equal amount of protein was used per sample. All subsequent steps were performed protected from direct light and in amber tubes. Blocking reagent provided in the kit was added, and samples were incubated for 30 min at 50 °C with regular vortexing. Proteins were subsequently precipitated using cold acetone to remove any trace of blocking reagent, and incubated at –20 °C for at least 30 min, followed by centrifugation at 3000g for 10 min at 4 °C. Protein pellets were resuspended in the labelling/reducing reagent provided and prepared as per the manufacturer's instructions. A combined protein sample was incubated with diluted dimethylformamide only as a negative control. Samples were incubated for 1 h at room temperature on a shaker. Proteins were acetone precipitated as above. Protein pellets were resuspended in wash buffer provided; a fraction of the protein extracts was kept aside as input to determine total Prdx2 levels. To pull down S-nitrosylated proteins, protein extracts were incubated overnight at 4 °C on a shaker with 50 μ l EZview streptavidin beads (Sigma). Beads were washed three times with wash buffer and resuspended in NuPAGE loading buffer supplemented with β -mercaptoethanol, and boiled for 5 min. Total protein (input) and S-nitrosylated proteins were run on pre-cast NuPAGE gels as per standard procedures. Results were expressed as intensity of signal for SNO-Prdx2 over total level of Prdx2 per sample.

For cells, cells transfected for 48 h and treated with either vehicle or SNOc were washed with PBS and scraped from the dish. After centrifugation at 1000 rpm for 5 min, cell pellets were resuspended directly in blocking reagent diluted in buffer A and incubated at 50 °C for 30 min. After centrifugation and subsequent acetone precipitation, protein pellets were resuspended in labelling/reducing reagent and incubated at room temperature for 1 h. After acetone precipitation, proteins were resuspended in wash buffer and quantified by BCA assay (Thermo Scientific). The subsequent steps are identical as for tissue above.

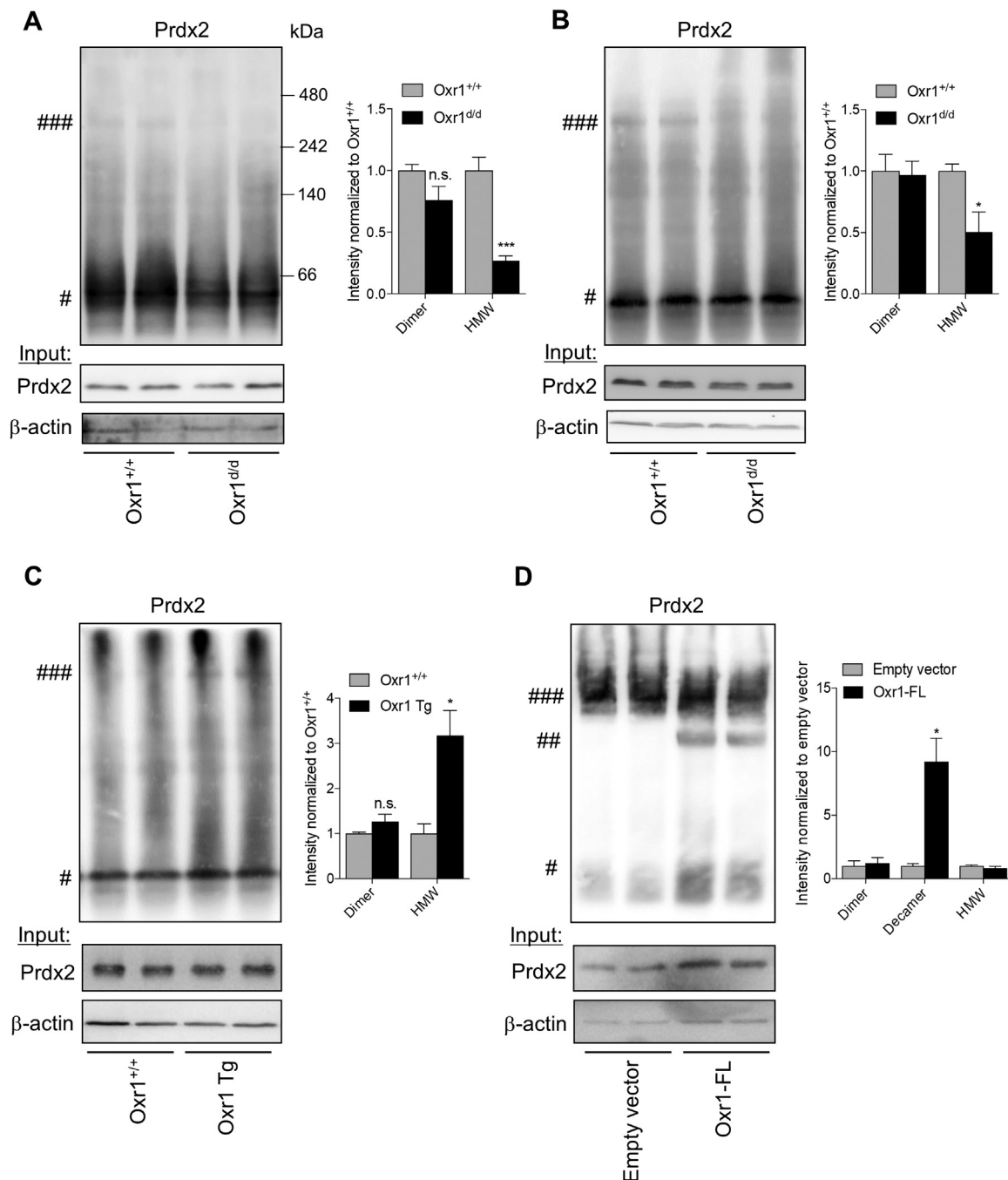


Fig. 1. Oxr1 plays a role in the regulation of the oligomerization status of Prdx2 *in vitro* and *in vivo*. (A–B) Representative western blot of Prdx2 from protein extracts of P18 wild-type control (Oxr1^{+/+}) and Oxr1^{d/d} brain tissue with the cerebellum removed (A) and the cerebellum alone (B). Quantification of the HMW Prdx2 complexes (###) and the Prdx2 dimer (#) is shown (N = 8 animals per group (A) and N = 3 (B)). (C) Western blot of Prdx2 from protein extracts of adult wild-type and Oxr1 Tg mouse brains without the cerebellum. Quantification of the HMW Prdx2 complexes and the dimer is shown (N = 3 animals per group). (D) Western blot of Prdx2 from protein extracts of N2A cells transfected with either an empty vector or Oxr1-FL and treated with 300 μ M H₂O₂ for 1 h. Quantification of the HMW Prdx2 complexes, the Prdx2 dimer (#) and the decamer (##) is shown (N = 3 independent repeats). For all panels, extracts were run on 10% BN-PAGE (native) gels and levels of Prdx2 and β -actin (input) were determined for the same samples, but run in reducing conditions on separate gels. β -actin was used as a loading control. Data are represented as mean \pm SEM. Panels A–D: t-test; *p < 0.05, ***p < 0.001.

2.10. Organomercury resin capture (ORC)

ORC from brain and cerebellum tissue was performed as previously described [40]. Briefly, samples were homogenized in homogenization buffer (250 mM HEPES free acid, 1 mM DTPA, 0.1 mM neocuproine, 1% Triton X-100, pH 7.7) using a tissue Precellys homogenizer (Bertin Corp.). Samples were clarified by centrifugation at full speed for 10 min at 4 °C and protein concentration was quantified by BCA assay (Thermo

Scientific). An equal amount of protein was used per sample. As a negative control a combined protein sample was incubated with the reducing agent DTT (10 mM) for 15 min at room temperature. Proteins were acetone precipitated and resuspended in blocking buffer (250 mM HEPES acid free, 1 mM DTPA, 0.1 mM neocuproine, 2.5% SDS, pH 7.7) supplemented with 50 mM blocking agent MMTS. Protein extracts were incubated for 30 min at 50 °C, with frequent vortexing, followed by acetone precipitation. Protein pellets were resuspended in loading

buffer (250 mM MES, 1 mM DTPA, 1% SDS, pH 6.0) and ready to be loaded on to the activated resin in glass columns; a fraction was kept aside as input. Organomercury resin (produced by the laboratory of Professor Harry Ischiropoulos University of Pennsylvania, USA and provided by Dr Mark Crabtree, University of Oxford) was washed and activated by consecutive washes with isopropanol, water, 0.1 M sodium bicarbonate pH 8.8, and equilibration buffer (50 mM NaCl, 50 mM MES, 1 mM DTPA, pH 6.0). After the resin was drained, samples were added and capped with 0.5 ml loading buffer and incubated at room temperature for 1 h protected from light to allow the reaction between S-nitrosylated proteins and the organomercury resin. The S-nitrosylated proteins cross-linked to the resin were then washed with consecutive 50 bed volumes of buffer A (50 mM Tris-HCl, 0.3 mM NaCl, 0.5% SDS, pH 7.5), buffer B (50 mM Tris-HCl, 0.3 mM NaCl, 0.05% SDS, pH 7.5), buffer C (50 mM Tris-HCl, 0.3 mM NaCl, 1% Triton X-100, 1 M urea, pH 7.5), and buffer D (50 mM Tris-HCl, 0.3 mM NaCl, 0.1% Triton X-100, 0.1 M urea, pH 7.5), followed by three washes of 200 bed volumes of water. Bound S-nitrosylated protein were then eluted by incubating the resin with 5% performic acid for 45 min at room temperature. The eluted proteins were precipitated by adding one volume of 100% TCA to four volumes of protein sample and incubated overnight at 4 °C. After centrifugation at full speed for 30 min at 4 °C, protein pellets were washed in cold acetone and resuspended in NuPAGE loading buffer supplemented with β -mercaptoethanol, and boiled for 5 min. Total protein (input) and S-nitrosylated proteins were run on pre-cast NuPAGE gels as per standard procedures. Results were expressed as intensity of signal for SNO-Prdx2 over total level of Prdx2 per sample.

2.11. Statistical analyses

Statistical analysis was performed using Prism software using one-way ANOVA or unpaired *t*-test. Data are presented as mean \pm SEM.

3. Results

3.1. *Oxr1* modulates the oligomerization state of the antioxidant enzyme Prdx2

It has been shown recently that *Oxr1* regulates the activity and degree of oligomerization of the multifunctional enzyme glucose-6-phosphate isomerase (GPI/Gpi1) via protein-protein interaction [27]. Therefore, seeing that *Oxr1* can influence ROS levels as well as protein multimer formation and aggregation, we tested the hypothesis that *Oxr1* is neuroprotective against O/N stress by regulating the function of essential proteins within these two pathways [26,28,36,41]. As a promising candidate interactor for *Oxr1*, we selected peroxiredoxin 2 (Prdx2) because it acts both as a chaperone and an antioxidant as well as being highly expressed in neurons [42–44]. Indeed, the expression patterns of Prdx2 and *Oxr1* overlap in the CNS, including the granule cell layer of the cerebellum [26,42,45]. Furthermore, similar to the knockout of *Oxr1*, loss of *Prdx2* in mice leads to accumulation of ROS and oxidative DNA damage, although this occurs in the CA1 region of the hippocampus as opposed to the cerebellum of *Oxr1* knockout mutants [46].

Given that the multiple functions of Prdx2 are regulated by its degree of oligomerization, we first tested whether *Oxr1* levels would affect Prdx2 oligomerization in the brain [47,48]. Using non-reducing native PAGE to preserve protein complexes, we assessed Prdx2 oligomerization in tissues from a constitutive *Oxr1* knockout mouse in which all isoforms of the protein are disrupted (*Oxr1*^{d/d}) [26–28]. Tissue samples were collected at a pre-symptomatic timepoint (P18), prior to the onset of neurodegeneration in this model. In wild-type (*Oxr1*^{+/+}) brain tissue, we observed a dimeric form of Prdx2 in addition to HMW complexes with an apparent molecular weight of approximately 400 kDa, as previously described (Fig. 1A) [48–50]. Interestingly, there was a significant decrease in these HMW Prdx2 complexes in the brain

of *Oxr1*^{d/d} mice compared to wild-type controls, both in the brain without the cerebellum (Fig. 1A) and in the cerebellum alone (Fig. 1B). To confirm that *Oxr1* levels regulate Prdx2 oligomerization, we next assessed the levels of Prdx2 multimers in brains from adult mice overexpressing an HA-tagged full-length *Oxr1* (*Oxr1*-FL) cDNA transgene (*Oxr1* Tg) [28]. Conversely to the observations from *Oxr1*^{d/d} knockout mice, levels of the HMW Prdx2 complexes were significantly increased in *Oxr1* Tg tissue compared to wild-type controls (Fig. 1C). Together, these data suggest that the levels of *Oxr1* modulate Prdx2 oligomerization *in vivo*. To validate that higher levels of *Oxr1* indeed favour higher-order Prdx2 complexes, we next analysed the degree of oligomerization of Prdx2 in cells over-expressing *Oxr1* and upon treatment with H₂O₂ to promote assembly of HMW Prdx2 complexes via Prdx2 overoxidation [48,50,51]. Interestingly, in cells over-expressing *Oxr1*-FL, specific HMW Prdx2 complexes were detected - namely its decameric species at the molecular weight of approximately 220 kDa - while this was not present in control vector-transfected cells (Fig. 1D). Overall, our data suggest that *Oxr1* is able to modulate Prdx2 oligomerization.

3.2. *Oxr1* interacts with the antioxidant enzyme Prdx2

To understand the mechanism by which *Oxr1* regulates the oligomerization of Prdx2, we next tested whether *Oxr1* and Prdx2 could interact. To assess binding between Prdx2 and *Oxr1*, we performed co-immunoprecipitation experiments in neuronal N2A cells co-expressing Prdx2 and either *Oxr1*-FL or the shortest *Oxr1* isoform (*Oxr1*-C). The latter isoform primarily consists of the TLDc domain, but is highly expressed in the brain and has a proven function as a neuroprotective protein [26,28]. Both *Oxr1* isoforms were found to co-immunoprecipitate with Prdx2 (Fig. 2A). The TLDc domain is common between both *Oxr1* isoforms, thus we went on to investigate whether this interaction would be maintained with other TLDc-containing proteins. We discovered that Prdx2 also interacts with full-length nuclear receptor coactivator 7 (Ncoa7-FL), and to a lesser extent with the shorter TLDc domain-containing isoform (Ncoa7-B) (Fig. 2A). We also observed binding to Tbc1d24, suggesting that Prdx2 is a common binding partner for most of the TLDc proteins (Fig. 2A). To investigate whether the *Oxr1* interaction occurs *in vivo*, we performed co-immunoprecipitation from wild-type mouse brain tissue and detected an interaction between endogenous *Oxr1* and Prdx2, confirming our *in vitro* data (Fig. 2B).

3.3. *Oxr1* and Prdx2 do not synergistically regulate H₂O₂-induced cell death

To investigate the significance of the *Oxr1*:Prdx2 interaction, we next tested systematically how *Oxr1* and Prdx2 might influence each other's functional roles. Both *Oxr1* and Prdx2 have been shown to be neuroprotective under oxidative stress; therefore, we quantified H₂O₂-induced cell death in a neuronal cell line expressing either *Oxr1*, Prdx2 or both proteins [26,52]. Consistent with previous reports, over-expression of *Oxr1*-FL, *Oxr1*-C or Prdx2 significantly reduced cell death under oxidative stress conditions; however, Prdx2 was significantly less protective than *Oxr1* in this assay (Fig. 2C) [26,28,53]. Co-expression of Prdx2 together with *Oxr1* did not alter significantly the neuroprotective properties of *Oxr1*.

Considering that Prdx2 can reduce H₂O₂ at a high kinetic rate, we next investigated whether the neuroprotection against oxidative stress that is conferred by *Oxr1* could be via regulation of Prdx2 activity [54,55]. To test this, we carried out a peroxide activity assay that measures reduction of H₂O₂ using purified recombinant proteins, and as expected, recombinant Prdx2 was able to dramatically reduce H₂O₂ levels (Fig. 2D) [37]. Recombinant *Oxr1*-C and *Oxr1*-FL were not, however, able to reduce H₂O₂ levels in this assay, similar to what has been observed previously (Fig. 2D) [28]. When Prdx2 and *Oxr1*-C were

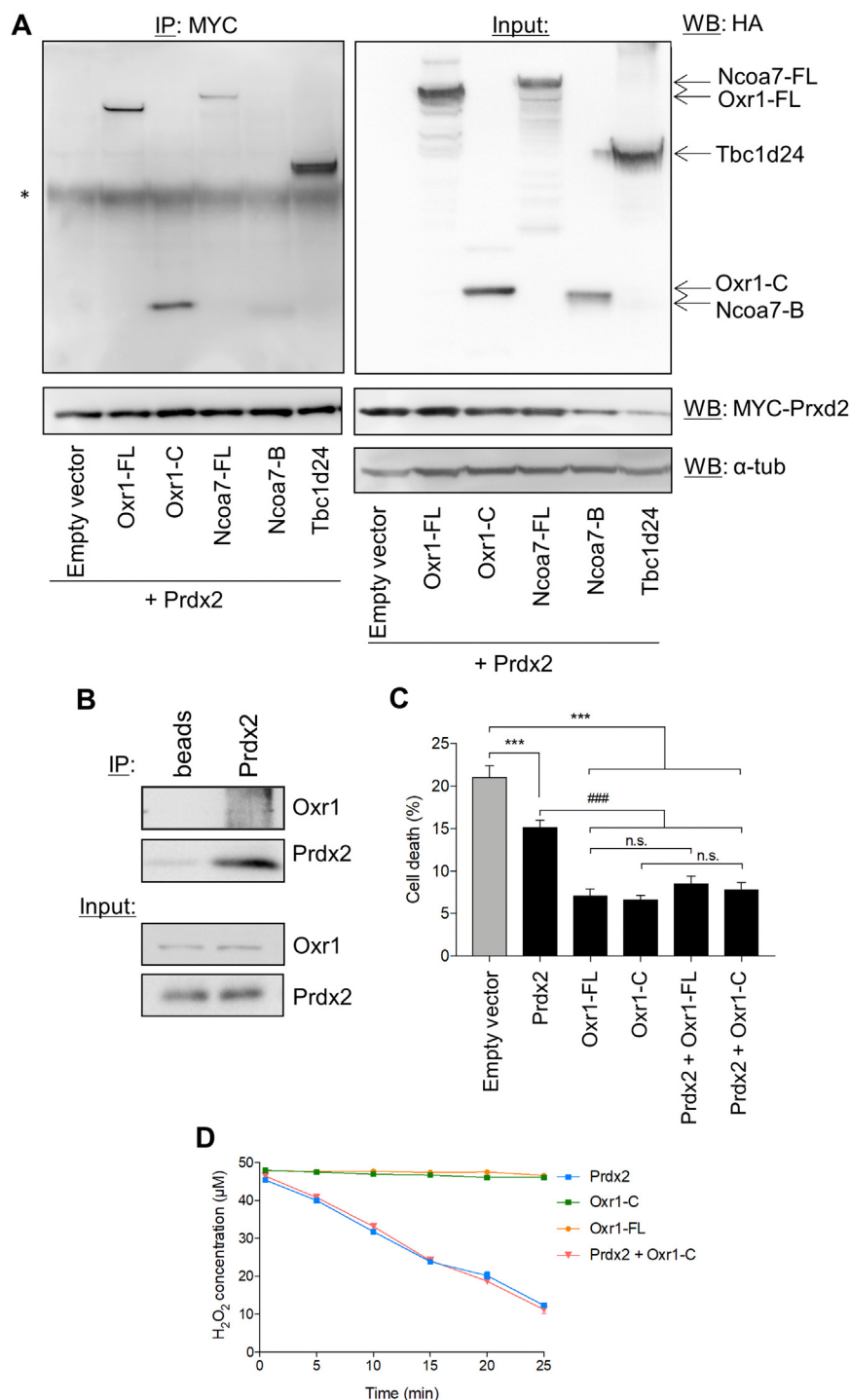


Fig. 2. Prdx2 binds to TLDc proteins, but does not interact functionally with Oxr1 to regulate H_2O_2 -induced cell death. (A) N2A cells were co-transfected with Prdx2-MYC and HA-tagged TLDc constructs as indicated and data from co-immunoprecipitations (IP) of the TLDc proteins using an anti-MYC antibody are shown by immunoblotting for HA (left panel). α -tubulin was used as a loading control for the input samples (right panel). The asterisk (*) represents non-specific IgG heavy chains. (B) Co-immunoprecipitation of Oxr1-FL with Prdx2 from adult wild-type mouse brain tissue (excluding the cerebellum). (C) N2A cells transfected with the indicated constructs were treated with 500 μ M H_2O_2 for 5 h and cell death was quantified as the number of pyknotic nuclei. 10 fields of view per condition were quantified ($N = 100$ –150 cells per field of view). (D) Changes in H_2O_2 concentration were monitored using a colorimetric ferrous oxidation-xylenol orange (FOX) assay over 25 min with either recombinant purified Prdx2, Oxr1-C, OXR1-FL or Prdx2 with Oxr1-C proteins with 50 μ M H_2O_2 . ($N = 3$ independent repeats). Data are represented as mean \pm SEM. Panel C: 1-way ANOVA; *** $p < 0.001$ compared to empty vectors, ### $p < 0.001$ compared to transfection with Prdx2.

incubated together, no enhancement in the rate of H_2O_2 decay was observed as compared to the rate observed for Prdx2 alone (Fig. 2D), suggesting that Prdx2 and Oxr1 do not interact synergistically to regulate cell death under oxidative stress or to reduce H_2O_2 levels.

3.4. Oxr1 and Prdx2 both modulate protein aggregation *in vitro*

As well as being an antioxidant enzyme, Prdx2 also possesses holdase activity [48,56]. Holdases are a class of chaperones that bind unfolded or misfolded molecules and prevent them from aggregating in an ATP-independent manner [17]. To investigate any functional interactions between Oxr1 and Prdx2 that may modulate Prdx2 chaperone

activity, we used a well-established *in vitro* aggregation assay with recombinant proteins. Insulin was induced to form large aggregates by incubation with DTT; its aggregation correlates with an increased turbidity of the reaction solution, which can be quantified by spectrophotometry [57]. Using this system, we observed a reduction in the aggregation of insulin in the presence of recombinant Prdx2, as expected, while lysozyme, a non-chaperone control, did not affect aggregation (Fig. 3A-C). Importantly, when Prdx2 was incubated with recombinant Oxr1-C, this led to a further significant reduction in insulin aggregation rate and in the aggregation at endpoint as compared to Prdx2 alone; this suggests that Oxr1-C may enhance the chaperone activity of Prdx2 (Fig. 3A-C). We confirmed these data by using a

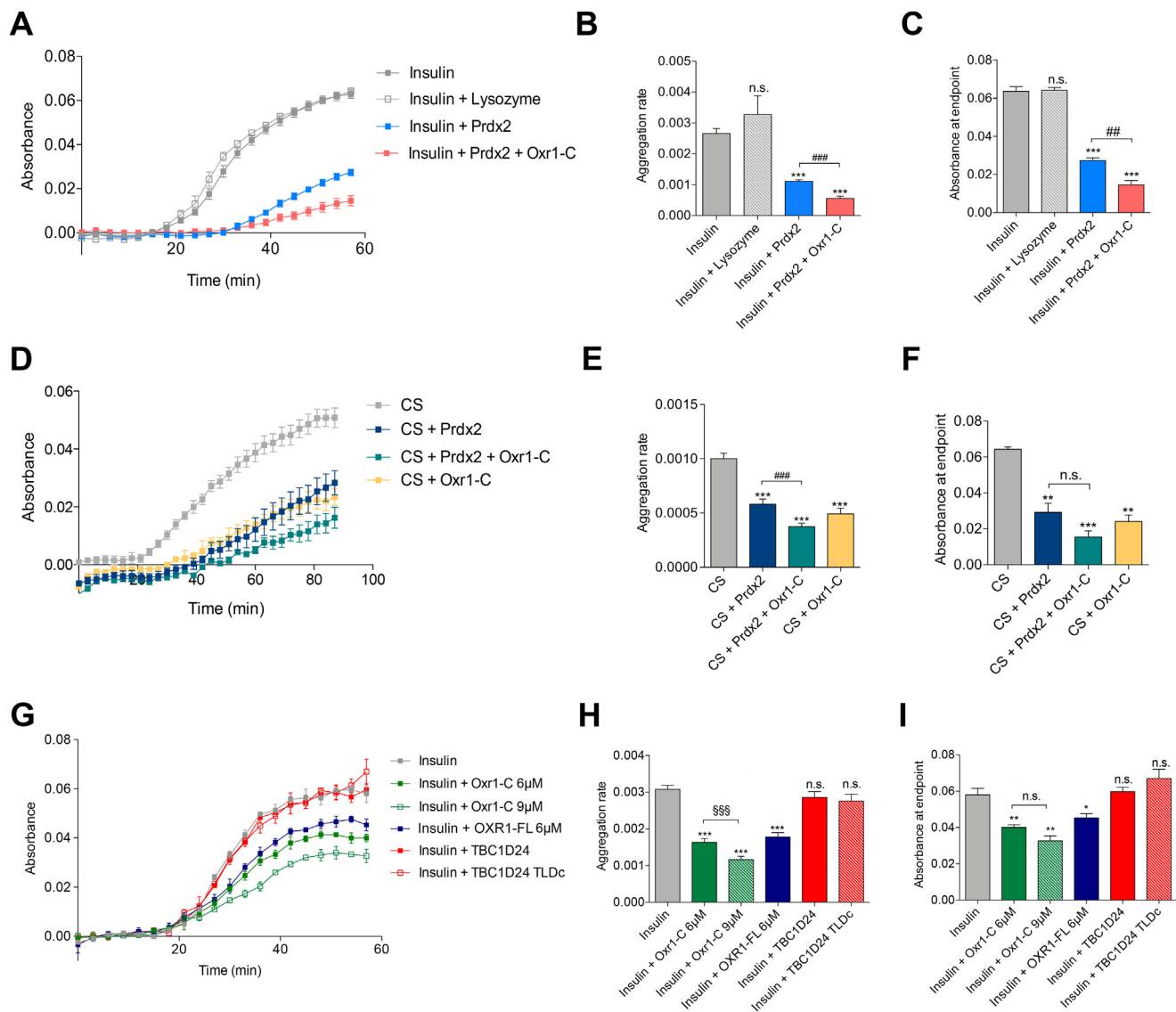


Fig. 3. Prdx2 and Oxr1 possess holdase activity. (A–C) DTT-induced insulin aggregation assay using recombinant Prdx2 and Oxr1-C with lysozyme as a negative control. Absorbance readings at 650 nm were taken every 3 min (A). Quantification of the aggregation rate (B) and absorbance at endpoint (C) are shown. (D–F) Thermally-induced citrate synthase (CS) aggregation assay using recombinant Prdx2 and Oxr1-C. Absorbance readings at 360 nm were taken every 3 min (D). Aggregation rate (E) and absorbance at end point (F) are shown. (G–I) DTT-induced insulin aggregation assay using two concentrations (6 μ M and 9 μ M) of recombinant Oxr1-C or human OXR1-FL (6 μ M), in parallel with human TBC1D24 and the TLDC domain of TBC1D24 (TBC1D24 TLDC). Absorbance readings at 650 nm were taken every 3 min (G). Quantification of the aggregation rate (H) and absorbance at endpoint (I) are presented. (A–I) All values are shown as normalized to the background signal. Data are represented as mean \pm SEM. B, C, H, I, E, F: *t*-test, **p* < 0.05, ***p* < 0.01, ****p* < 0.001 as compared to insulin (B, C, H, I) or CS (E, F), ##*p* < 0.01, ###*p* < 0.001 as compared to insulin + Prdx2 (B, C, H, I) or CS + Prdx2 (E, F), §§§*p* < 0.001 as compared to insulin + Oxr1-C 6 μ M (H, I).

second aggregation assay that utilises thermally-induced aggregation of citrate synthase (CS). In agreement with the insulin aggregation data, the presence of Prdx2 reduced the thermally-induced aggregation of CS, and the rate of aggregation was significantly reduced further when Prdx2 was co-incubated with Oxr1-C (Fig. 3D–F).

Surprisingly, when these assays were performed with Oxr1-C only, we detected a significant reduction of approximately 50% in both the chemically- and thermally-induced aggregation rate of insulin and CS (Fig. 3D–I). Given that these assays are cell-free, these data are not reliant on other proteins, thus suggesting that Oxr1-C possesses a potential holdase activity. To confirm this observation, we tested whether increasing Oxr1-C concentration would lead to an increase in protective activity against chemically-induced protein aggregation. We did observe a significant decrease in substrate aggregation rate as well as a slight reduction in the aggregation at end point with an increased concentration of Oxr1-C, further supporting a chaperone activity for

Oxr1-C (Fig. 3G–I).

As the Oxr1-C isoform is mainly comprised of the TLDC domain, our data indicate that the chaperone activity we observe may be conserved in other TLDC-containing proteins. To test this hypothesis, we quantified the chaperone activity of full-length OXR1 (OXR-FL) and TBC1D24 using the chemically-induced protein aggregation assay. Using a recombinant OXR1-FL, we detected a significant reduction in both the aggregation rate and aggregation at end point compared to the control, suggesting that OXR1-FL also possesses holdase activity (Fig. 3G–I). Interestingly, we did not detect any reduction in the formation of insulin aggregates when incubated with full-length TBC1D24, suggesting that TBC1D24 does not possess holdase activity (Fig. 3G–I). We performed a similar experiment using a recombinant protein constituted of only the C-terminal TLDC domain of TBC1D24. Similar to full-length TBC1D24, the TLDC domain alone did not show any chaperone activity (Fig. 3G–I). Therefore, we have identified a novel activity for Oxr1 as a

potential holdase that is likely not conserved with the related TLDC protein TBC1D24.

3.5. *Oxr1* modulates Prdx2 post-translational modifications (PTMs)

Prdx2 function is regulated by its level of oligomerization and through PTMs such as overoxidation and S-nitrosylation, in addition to conformational changes [48,58–60]. In particular, reversible oxidation of catalytic cysteine residues occurs during the catalytic cycle of Prdx2: in the presence of low levels of H_2O_2 , Prdx2 is oxidised and reactivated, while under high levels of H_2O_2 , its cysteine residues are overoxidized, forming sulfinic and sulfonic acid (Prdx-SO_{2/3}), which inactivates its antioxidant activity but stabilizes the HMW complexes which drive its chaperone activity [48,51,61]. Given our findings that *Oxr1* levels modulate Prdx2 oligomerization, we next investigated whether *Oxr1* could affect Prdx2 overoxidation. We first assessed overoxidation of endogenous Prdx2 *in vitro* by quantifying the levels of Prdx2-SO_{2/3} over the total level of Prdx2 from H_2O_2 -treated cells. Using an antibody that recognises overoxidized Prdx1, Prdx2, Prdx3 and Prdx4, we confirmed previously reported overoxidation of the aforementioned Prdxs induced by H_2O_2 treatment [62]. Interestingly, under these conditions, levels of Prdx2 overoxidation were significantly higher in cells overexpressing *Oxr1*-FL (Fig. 4A) and a similar effect was observed in cells overexpressing *Oxr1*-C (Fig. 4B). This suggests that *Oxr1* modulates, directly or indirectly, Prdx2 overoxidation. We next tested if levels of *Oxr1* would similarly affect overoxidation of Prdx2 *in vivo* by using the cerebellum and the remaining brain tissue from *Oxr1* Tg mice or control littermates. Similar to what we observed *in vitro* in *Oxr1* over-expressing cells, a significant increase in Prdx2 overoxidation levels in brain of transgenic animals were detectable as compared to wild-type mice (Fig. 4C). There was also a significant increase in Prdx2-SO_{2/3} levels in cerebellar tissue from *Oxr1* Tg mice (Fig. 4D). To further investigate the role of *Oxr1* in regulating Prdx2 overoxidation, we analysed the levels of Prdx-SO_{2/3} in brains from *Oxr1*^{d/d} mice as compared to controls at the presymptomatic P18 timepoint. We did not observe any significant changes in Prdx2 overoxidation in the brain (Fig. 4E); however, levels of Prdx2-SO_{2/3} were significantly reduced in cerebella from *Oxr1*^{d/d} animals as compared to controls (Fig. 4F). These data suggest that *Oxr1* regulates levels of Prdx2 overoxidation; interestingly, this occurs differentially in the cerebellum – the site of neurodegeneration in the *Oxr1*^{d/d} mutant – as compared to the rest of the brain.

S-nitrosylation is another essential PTM regulating Prdx2 function. Indeed, addition of an NO group at its cysteine residues has been shown to reduce the antioxidant activity of Prdx2 [58]. To test whether *Oxr1* would have an effect on Prdx2 S-nitrosylation *in vitro*, we used a neuronal cell line SH-SY5Y treated with the physiological cell-permeable NO-donor, S-nitrosocysteine (SNOC), to induce S-nitrosylation of proteins. Using a biotin switch assay, we quantified levels of S-nitrosylated endogenous PRDX2 (SNO-PRDX2) and found that cells treated with SNOC show a significant increase in levels of SNO-PRDX2, as previously described (Fig. 5A) [58]. However, both in vehicle- and SNOC-treated conditions, the levels of SNO-PRDX2 were significantly reduced when cells were over-expressing *Oxr1*-FL or *Oxr1*-C as compared to control cells suggesting that *Oxr1* reduces SNO-Prdx2 levels (Fig. 5A). To test whether similar observations could be made *in vivo*, we quantified the levels of SNO-Prdx2 in brain and cerebellum extracts from *Oxr1* Tg mice and wild-type controls. While levels of SNO-Prdx2 in the brain were slightly decreased without reaching significance (Fig. 5B), we showed a significant reduction in the levels of SNO-Prdx2 in the cerebella of *Oxr1* Tg mice as compared to controls (Fig. 5C). To investigate further whether levels of *Oxr1* modulate SNO-Prdx2, we next quantified the levels of SNO-Prdx2 in *Oxr1*^{d/d} mice using two different approaches: first, the originally described biotin switch method to detect SNO-proteins, that converts S-nitrosylated residues to biotinylated cysteines which are then immunoprecipitated by streptavidin beads, and second, a newly developed approach, organomercury resin capture (ORC) that

relies on the selective and semi-stable reaction of S-nitrosylated residues with phenylmercury compounds of an organomercury resin [40,63]. We showed that SNO-Prdx2 levels were similar in the brain of *Oxr1*^{d/d} and control animals, using either the biotin switch or ORC approach (Fig. 5D and 5F). In contrast, a significant increase in the levels of SNO-Prdx2 was seen with both approaches in cerebella of *Oxr1*^{d/d} mice as compared to controls (Fig. 5E and 5G) suggesting that *Oxr1* participates in the modulation of Prdx2 S-nitrosylation in the cerebellum. Together, we have shown that *Oxr1* modulates two essential Prdx2 PTMs, overoxidation and S-nitrosylation.

4. Discussion

Our current study sheds new light on the molecular mode of action of *Oxr1* as a functional switch for the essential antioxidant and chaperone Prdx2. Indeed, we show that *Oxr1* modulates oligomerization of HMW Prdx2 chaperone complexes and key PTMs regulating the dual functions of Prdx2.

Our study is in accordance with our previous observations that *Oxr1* reduces aggregation of the mutated ALS-associated TDP-43 and FUS proteins in cellular models of ALS; this process relies on the interaction between *Oxr1* and TDP-43 or FUS, but is independent of the proteasome or autophagy [36]. Based on our current findings, we hypothesise that *Oxr1* may reduce protein aggregation first through its chaperone activity and second by favoring the formation of HMW Prdx2 chaperone complexes. Another key function described for *Oxr1* is its ability to reduce levels of ROS and oxidative stress markers in oxidative stress-treated neurons as well as in SOD1^{G93A} ALS mouse model [26,29]. However, *Oxr1* has no direct catalytic activity, thus it has remained unclear how *Oxr1* could carry out this role. Here, we showed that *Oxr1* regulates the activity of the antioxidant protein Prdx2, in particular, by modulating two key PTMs of Prdx2, its overoxidation and S-nitrosylation: loss of *Oxr1* increases SNO-Prdx2 and reduces its overoxidation, while increasing *Oxr1* levels leads to the opposite effect. This is significant because these PTMs regulate Prdx2 antioxidant activity and are intertwined: S-nitrosylation of Prdx2 reduces its H_2O_2 -induced overoxidation and inhibits its antioxidant activity [58]. By affecting both the degree of oligomerization and the PTMs of Prdx2, *Oxr1* could potentially fine-tune the amount of peroxidases versus chaperones in cells. A slight shift in this proportion could have a major impact on the global cell function given that Prdxs represent 0.2–0.8% of the total soluble protein fraction in cells and tissues, and that Prdx2 is highly expressed in neurons [42–44,64]. Therefore, *Oxr1* may indirectly regulate the levels of oxidative stress in cells by modulating the PTMs of Prdx2 and subsequently fine-tuning its antioxidant activity. This newly described function is likely to run in concert with the proposed role for *Oxr1* as a regulator of antioxidant gene expression, this latter regulatory hypothesis being supported by a number of studies that have combined *OXR1* knock-down with genome-wide or targeted transcriptomics [30,33]. Further work is required to understand the molecular mechanisms involved, although there is evidence that gene modulation via p53-associated pathways is more plausible than *Oxr1* acting upstream of the antioxidant Nrf2 signaling cascade [30,31].

The current study also provides an insight into the link between loss of *Oxr1* and cellular degeneration in the cerebellum of the *Oxr1*^{d/d} mouse [28]. We observed higher levels of SNO-Prdx2 and reduced levels of Prdx2-SO_{2/3} in the neurodegenerative *Oxr1* knockout mouse at a presymptomatic stage, specifically in the cerebellum – the only brain region affected in this mutant – suggesting that aberrant PTM of Prdx2 may participate in the neurodegeneration observed in this mouse. Importantly, SNO-Prdx2 breaks the normal redox cycle that regenerates Prdx2, inhibiting Prdx2 antioxidant activity and leading to high levels of oxidative stress in cells [58]. Increased levels of SNO-Prdx2 have been observed in the brain of the PQ/MB-exposed PD mouse model, as well as in dopaminergic neurons differentiated from induced pluripotent stem cells from PD patients and in *post mortem* brains of PD

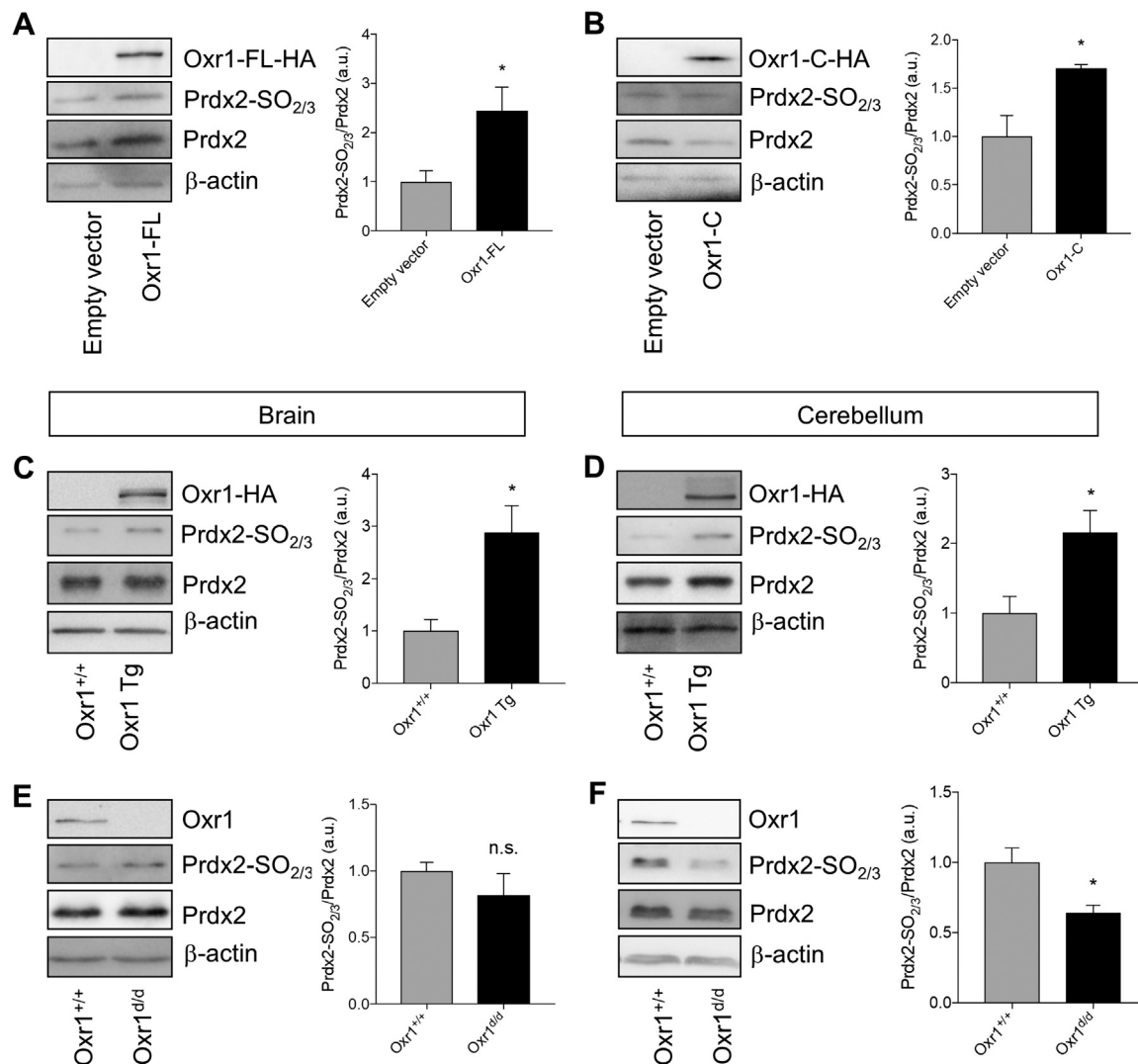


Fig. 4. Oxr1 modulates overoxidation of Prdx2 catalytic residues *in vitro* and *in vivo*. (A-B) N2A cells were transfected with either Oxr1-FL (A) or Oxr1-C (B) and treated with 300 μM H₂O₂ for 1 h. Representative image of western blots and quantification of Prdx2 overoxidation is shown as the ratio of Prdx2-SO_{2/3} to total Prdx2 (N = 6 independent repeats for Oxr1-FL and N = 3 independent repeats for Oxr1-C). (C-F) Representative westerns blots of protein extracts from an adult Oxr1 overexpressing mouse (Oxr1 Tg) (C-D) and a P18 Oxr1 knockout (Oxr1^{d/d}) mouse (E-F) from both the brain lacking the cerebellum and cerebellar tissues, with quantification of Prdx2 overoxidation compared to wild-type controls (N = 3–4 animals per group). β-actin was used as a loading control. Data presented as mean ± SEM. Panels A-F: *t*-test; **p* < 0.05.

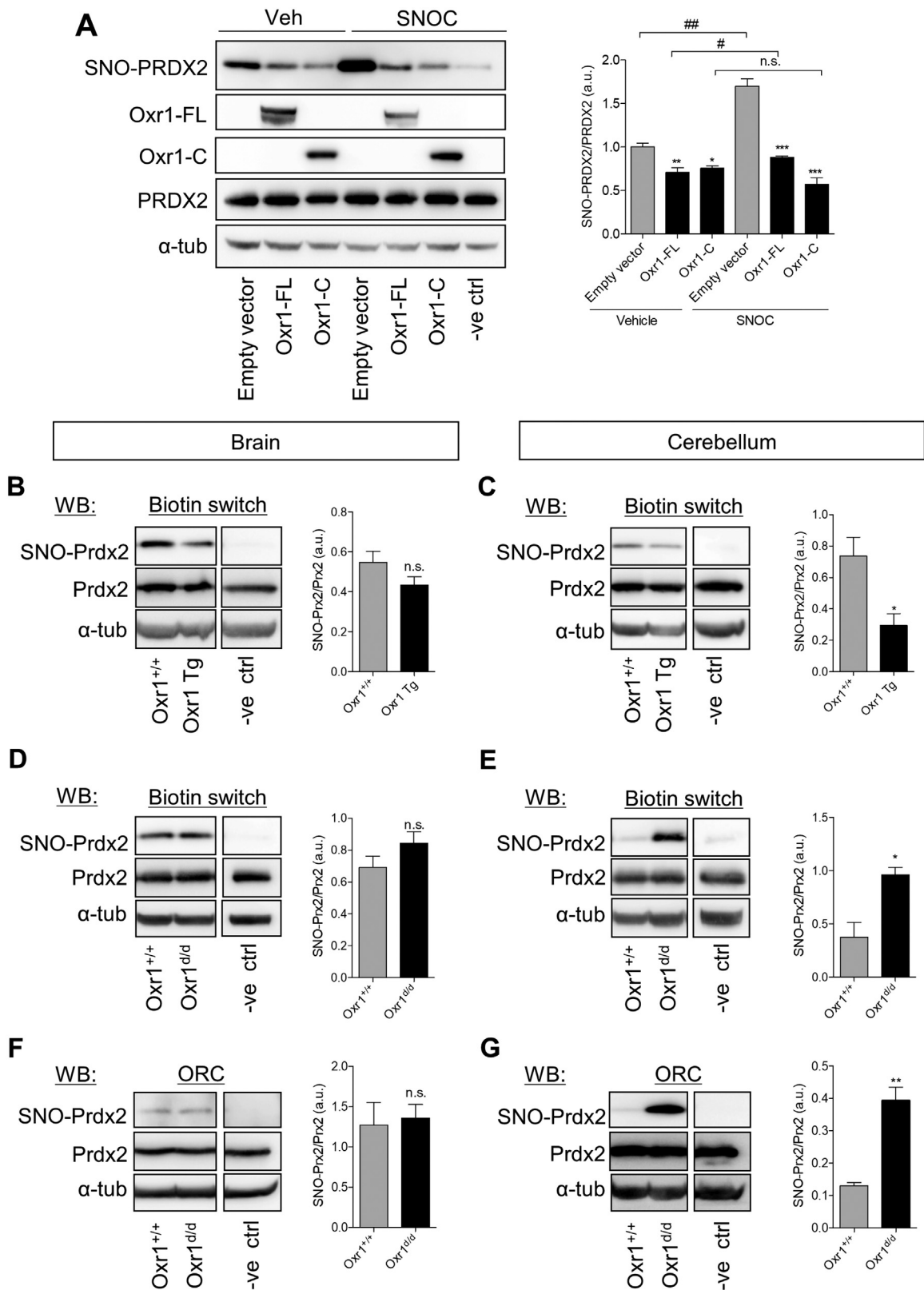
patients, suggesting that SNO-Prdx2 participates in the neurodegenerative process [58,65]. It was also shown *in vitro* that S-nitrosylation of Prdx2 led to a reduction of Prdx2-SO_{2/3} and of its neuroprotective function against H₂O₂-induced apoptosis [58]. Therefore, our current model is that loss of Oxr1 in the knockout mouse model impairs Prdx2 chaperone activity through reduction of HMW Prdx2 chaperone complexes and reduction of the complexes-stabilising PTM, Prdx2-SO_{2/3}. In addition, Prdx2 antioxidant activity is also inactivated by the increase in S-nitrosylation of Prdx2. These changes in PTMs being cerebellum-specific, this may lead to a detrimental increase in protein aggregation and oxidative stress in the cerebellum, precipitating the degeneration of the cerebellar granule cells in Oxr1 knockout animals. Of note, we focused here on overoxidation and S-nitrosylation of Prdx2; however, Prdx2 function can be affected by other PTMs, such as phosphorylation and nitration, which have also been involved in neurodegeneration [66].

Using two *in vitro* assay systems, we have discovered that Oxr1-C and OXR1-FL possess a potential holdase activity. Because Oxr1-C is almost exclusively constituted of the TLDc domain, we tested whether this function was shared with another TLDc-containing protein.

Surprisingly, however, TBC1D24 did not possess any holdase activity; neither the full-length protein nor the TLDc domain alone. This interesting finding indicates that, although all TLDc-containing proteins are neuroprotective, they may also carry out their own specific functions [23]. This may be driven in part by key residues in the TLDc domain that are yet to be identified. Importantly, we also showed that Tbc1d24 interacts with Prdx2, suggesting that the holdase activity is independent of the ability to bind Prdx2. Here, we have focused on the interplay between Oxr1 and Prdx2; yet the fact that Prdx2 has the ability to bind to other TLDc-containing proteins suggests that functional compensation and competition with other TLDc proteins may play a part, and would require further investigation.

5. Conclusions

In summary, our study not only discovered a new function for Oxr1 as a potential holdase, it also identified a novel mode of action for Oxr1, acting on the oxidative stress response and protein aggregation by modulating the oligomerization and PTMs of the fundamental antioxidant enzyme Prdx2. Our study also places Oxr1 at the intersection



(caption on next page)

between two key pathways involved in the neurodegenerative process.

Acknowledgments

The research leading to these results has received funding from the

European Research Council under the European Union's Seventh Framework Programme (FP7/2007–2013)/ERC grant agreement number 311394/“PAROSIN” to PLO and supporting PLO, MJF and DMS, and from the John Fell Oxford University Press (OUP) Research Fund (to MF - PLO, JS, and MC co-PI). We thank Professor Harry

Fig. 5. Oxr1 regulates S-nitrosylation of Prdx2 *in vitro* and *in vivo* in the cerebellum. (A) SH-SY5Y cells were treated for 30 min with 200 μ M SNO or vehicle (veh) and processed for the biotin switch assay to quantify the levels of S-nitrosylated endogenous PRDX2 (SNO-PRDX2) by western blot in the presence of the constructs as indicated. (N = 3 independent repeats). (B–C) Representative western blots of SNO-Prdx2 levels in brain (B) or cerebellum (C) as determined by biotin switch from mice over-expressing Oxr1 (Oxr1 Tg) compared to wild-type controls (Oxr1^{+/+}) (N = 3 animals per group). (D–E) SNO-Prdx2 levels in brain (D–F) or cerebellum (E–G) determined by biotin switch (D–E) or organomercury resin capture (ORC, F–G) from Oxr1 knockout (Oxr1^{0/0}) mice compared to wild-type controls (N = 3 animals per group). In all panels, quantification is shown as the ratio of SNO-Prdx2 to total Prdx2 with α -tubulin used as a loading control. Data presented as mean \pm SEM. Negative controls (-ve Ctrl) were combined proteins diluted in dimethylformamide without labelling/reducing reagent (for biotin switch) or proteins incubated with 10 mM DTT for 15 min (for ORC). Panel A: 1-way ANOVA (comparison of constructs to empty vector in either vehicle or SNO-treated condition) and *t*-test (comparison of each construct between vehicle and SNO-treated conditions), Panels B–G: *t*-test; **p* < 0.05, ***p* < 0.01, ****p* < 0.001 as compared to empty vector-transfected cells or to control mice, #*p* < 0.05, ##*p* < 0.01 as compared to vehicle treated cells.

Ischiropoulos and Dr Paschalis-Thomas Doulias, University of Pennsylvania, USA for producing the organomercury resin.

Appendix A. Supplementary material

Supplementary data associated with this article can be found in the online version at doi:10.1016/j.freeradbiomed.2018.10.447.

References

- [1] L.G. Apostolova, Alzheimer's disease, *Continuum* 22 (2) (2016) 419–434.
- [2] A. Chio, G. Logroscino, B.J. Traynor, J. Collins, J.C. Simeone, L.A. Goldstein, L.A. White, Global epidemiology of amyotrophic lateral sclerosis: a systematic review of the published literature, *Neuroepidemiology* 41 (2) (2013) 118–130.
- [3] S.J. Evans, I. Douglas, M.D. Rawlins, N.S. Wexler, S.J. Tabrizi, L. Smeeth, Prevalence of adult Huntington's disease in the UK based on diagnoses recorded in general practice records, *J. Neurol. Neurosurg. Psychiatry* 84 (10) (2013) 1156–1160.
- [4] J.K. Andersen, Oxidative stress in neurodegeneration: cause or consequence? *Nat. Med.* 10 Suppl. (2004) S18–S25.
- [5] K.K. Chung, K.K. David, Emerging roles of nitric oxide in neurodegeneration, *Nitric Oxide* 22 (4) (2010) 290–295.
- [6] D.P. Jones, Radical-free biology of oxidative stress, *Am. J. Physiol. Cell Physiol.* 295 (4) (2008) C849–C868.
- [7] J. Navarro-Yepes, L. Zavala-Flores, A. Anandhan, F. Wang, M. Skotak, N. Chandra, M. Li, A. Pappa, D. Martinez-Fong, L.M. Del Razo, B. Quintanilla-Vega, R. Franco, Antioxidant gene therapy against neuronal cell death, *Pharmacol. Ther.* 142 (2) (2014) 206–230.
- [8] T.T. Reed, W.M. Pierce Jr., D.M. Turner, W.R. Markesbery, D.A. Butterfield, Proteomic identification of nitrated brain proteins in early Alzheimer's disease inferior parietal lobule, *J. Cell. Mol. Med.* 13 (8B) (2009) 2019–2029.
- [9] T.T. Reed, Lipid peroxidation and neurodegenerative disease, *Free Radic. Biol. Med.* 51 (7) (2011) 1302–1319.
- [10] Y. Chang, Q. Kong, X. Shan, G. Tian, H. Ilieva, D.W. Cleveland, J.D. Rothstein, D.R. Borchelt, P.C. Wong, C.L. Lin, Messenger, RNA oxidation occurs early in disease pathogenesis and promotes motor neuron degeneration in ALS, *PLOS One* 3 (8) (2008) e2849.
- [11] B. Halter, J.L. Gonzalez de Aguilar, F. Rene, S. Petri, B. Fricker, A. Echaniz-Laguna, L. Dupuis, Y. Larnet, J.P. Loeffler, Oxidative stress in skeletal muscle stimulates early expression of Rad in a mouse model of amyotrophic lateral sclerosis, *Free Radic. Biol. Med.* 48 (7) (2010) 915–923.
- [12] D. Hartl, V. Schuldt, S. Forler, C. Zabel, J. Klose, M. Rohe, Presymptomatic alterations in energy metabolism and oxidative stress in the APP23 mouse model of Alzheimer disease, *J. Proteome Res.* 11 (6) (2012) 3295–3304.
- [13] M.S. Medeiros, A. Schumacher-Schuh, A.M. Cardoso, G.V. Bochi, J. Baldissarelli, A. Kegler, D. Santana, C.M. Chaves, M.R. Schetinger, R.N. Moresco, C.R. Rieder, M.R. Figuera, Iron and oxidative stress in Parkinson's disease: an observational study of injury biomarkers, *PLOS One* 11 (1) (2016) e0146129.
- [14] A. Skoumalova, J. Hort, Blood markers of oxidative stress in Alzheimer's disease, *J. Cell. Mol. Med.* 16 (10) (2012) 2291–2300.
- [15] P.K. Andrus, T.J. Fleck, M.E. Gurney, E.D. Hall, Protein oxidative damage in a transgenic mouse model of familial amyotrophic lateral sclerosis, *J. Neurochem.* 71 (5) (1998) 2041–2048.
- [16] I. Lindberg, J. Shorter, R.L. Wiseman, F. Chiti, C.A. Dickey, P.J. McLean, Chaperones in neurodegeneration, *J. Neurosci.* 35 (41) (2015) 13853–13859.
- [17] R.U. Mattoo, P. Goloubinoff, Molecular chaperones are nanomachines that catalytically unfold misfolded and alternatively folded proteins, *Cell. Mol. Life Sci.* 71 (17) (2014) 3311–3325.
- [18] L. De Mena, E. Coto, E. Sanchez-Ferrero, R. Ribacoba, L.M. Guisasaola, C. Salvador, M. Blazquez, V. Alvarez, Mutational screening of the mortalin gene (HSPA9) in Parkinson's disease, *J. Neural Transm.* 116 (10) (2009) 1289–1293.
- [19] R. Wadhwa, J. Ryu, H.M. Ahn, N. Saxena, A. Chaudhary, C.O. Yun, S.C. Kaul, Functional significance of point mutations in stress chaperone mortalin and their relevance to Parkinson disease, *J. Biol. Chem.* 290 (13) (2015) 8447–8456.
- [20] M.E. Conway, M. Harris, S-nitrosylation of the thioredoxin-like domains of protein disulfide isomerase and its role in neurodegenerative conditions, *Front. Chem.* 3 (2015) 27.
- [21] G.S. Jeon, T. Nakamura, J.S. Lee, W.J. Choi, S.W. Ahn, K.W. Lee, J.J. Sung, S.A. Lipton, Potential effect of S-nitrosylated protein disulfide isomerase on mutant SOD1 aggregation and neuronal cell death in amyotrophic lateral sclerosis, *Mol. Neurobiol.* 49 (2) (2014) 796–807.
- [22] M.R. Volkert, N.A. Elliott, D.E. Housman, Functional genomics reveals a family of eukaryotic oxidation protection genes, *Proc. Natl. Acad. Sci. USA* 97 (26) (2000) 14530–14535.
- [23] M.J. Finelli, P.L. Oliver, TLDc proteins: new players in the oxidative stress response and neurological disease, *Mamm. Genome: Off. J. Int. Mamm. Genome Soc.* 28 (9–10) (2017) 395–406.
- [24] S. Balestrini, M. Milh, C. Castiglioni, K. Luthy, M.J. Finelli, P. Verstreken, A. Cardon, B.G. Strazisar, J.L. Holder Jr., G. Lesca, M.M. Mancardi, A.L. Poulat, G.M. Repetto, S. Banka, L. Bilo, L.E. Birkeland, F. Bosch, K. Brockmann, J.H. Cross, D. Doummar, T.M. Felix, F. Giuliano, M. Hori, I. Huning, H. Kayserili, U. Kini, M.M. Lees, G. Meenakshi, L. Mewasingh, A.T. Pagnamenta, S. Peluso, A. Mey, G.M. Rice, J.A. Rosenfeld, J.C. Taylor, M.M. Troester, C.M. Stanley, D. Ville, M. Walkiewicz, A. Falace, A. Fassio, J.R. Lemke, S. Bishop, J. Tardif, N.F. Ajeawung, A. Tolun, M. Corbett, J. Gecz, Z. Afawi, K.B. Howell, K.L. Oliver, S.F. Berkovic, I.E. Scheffer, F.A. de Falco, P.L. Oliver, P. Striano, F. Zara, P.M. Campeau, S.M. Sisodiya, TBC1D24 genotype-phenotype correlation: epilepsies and other neurologic features, *Neurology* 87 (1) (2016) 77–85.
- [25] M.J. Finelli, D. Aprile, E. Castroflorio, A. Jeans, M. Moschetta, L. Chessum, M.T. Degiacomi, J. Grassegger, A. Lupien-Meilleur, A. Bassett, E. Rossignol, P.M. Campeau, M.R. Bowl, F. Benfenati, A. Fassio, P.L. Oliver, The epilepsy-associated protein TBC1D24 is required for normal development, survival and vesicle trafficking in mammalian neurons, *Hum. Mol. Genet.* (2018) (ddy370-ddy370).
- [26] M.J. Finelli, L. Sanchez-Pulido, K.X. Liu, K.E. Davies, P.L. Oliver, The evolutionarily conserved Tre2/Bub2/Cdc16 (TBC), Lysin Motif (LysM), Domain Catalytic (TLDc) domain is neuroprotective against oxidative stress, *J. Biol. Chem.* 291 (6) (2016) 2751–2763.
- [27] M.J. Finelli, T. Paramo, E. Pires, B.J. Ryan, R. Wade-Martins, P.C. Biggin, J. McCullagh, P.L. Oliver, Oxidation resistance 1 modulates glycolytic pathways in the cerebellum via an interaction with glucose-6-phosphate isomerase, *Mol. Neurobiol.* (2018), <https://doi.org/10.1007/s12035-018-1174-x>.
- [28] P.L. Oliver, M.J. Finelli, B. Edwards, E. Bitoun, D.L. Butts, E.B. Becker, M.T. Cheeseman, B. Davies, K.E. Davies, Oxr1 is essential for protection against oxidative stress-induced neurodegeneration, *PLOS Genet.* 7 (10) (2011) e1002338.
- [29] K.X. Liu, B. Edwards, S. Lee, M.J. Finelli, B. Davies, K.E. Davies, P.L. Oliver, Neuron-specific antioxidant OXR1 extends survival of a mouse model of amyotrophic lateral sclerosis, *Brain* 138 (Pt 5) (2015) 1167–1181.
- [30] M. Yang, X. Lin, A. Rowe, T. Rognes, L. Eide, M. Björås, Transcriptome analysis of human OXR1 depleted cells reveals its role in regulating the p53 signaling pathway, *Sci. Rep.* 30 (5) (2015).
- [31] M. Yang, L. Luna, J.G. Sørbo, I. Alseth, R.F. Johansen, P.H. Backe, N.C. Danbolt, L. Eide, M. Björås, Human OXR1 maintains mitochondrial DNA integrity and counteracts hydrogen peroxide-induced oxidative stress by regulating antioxidant pathways involving p21, *Free Radic. Biol. Med.* 77 (0) (2014) 41–48.
- [32] X. Zhang, S. Zhang, X. Liu, Y. Wang, J. Chang, X. Zhang, S.G. Mackintosh, A.J. Tackett, Y. He, D. Lv, R.-M. Laberge, J. Campisi, J. Wang, G. Zheng, D. Zhou, Oxidation resistance 1 is a novel senolytic target, *Aging Cell* 17 (4) (2018) (e12780-e12780).
- [33] G. Jaramillo-Gutierrez, A. Molina-Cruz, S. Kumar, C. Barillas-Mury, The Anopheles gambiae oxidation resistance 1 (OXR1) gene regulates expression of enzymes that detoxify reactive oxygen species, *PLOS One* 5 (6) (2010) e11168.
- [34] M. Blaise, H.M. Alsarraf, J.E. Wong, S.R. Midtgard, F. Laroche, L. Schack, H. Spaink, J. Stougaard, S. Thirup, Crystal structure of the TLDc domain of oxidation resistance protein 2 from zebrafish, *Proteins* 80 (6) (2012) 1694–1698.
- [35] Y. Sanada, S. Asai, A. Ikemoto, T. Moriwaki, N. Nakamura, M. Miyaji, Q.M. Zhang-Akiyama, Oxidation resistance 1 is essential for protection against oxidative stress and participates in the regulation of aging in *Caenorhabditis elegans*, *Free Radic. Res.* 48 (8) (2014) 919–928.
- [36] M.J. Finelli, K.X. Liu, Y. Wu, P.L. Oliver, K.E. Davies, Oxr1 improves pathogenic cellular features of ALS-associated FUS and TDP-43 mutations, *Hum. Mol. Genet.* 24 (12) (2015) 3529–3544.
- [37] S. Yan, S. Chen, Z. Li, H. Wang, T. Huang, X. Wang, J. Wang, Biochemical characterization of human peroxiredoxin 2, an antioxidant protein, *Acta Biochim. Biophys. Sin.* 44 (9) (2012) 759–764.
- [38] K.J. Nelson, D. Parsonage, Measurement of peroxiredoxin activity, *Curr. Protoc. Toxicol.* (2011) (Chapter 7: Unit7.10).
- [39] S.R. Jaffrey, H. Erdjument-Bromage, C.D. Ferris, P. Tempst, S.H. Snyder, Protein S-nitrosylation: a physiological signal for neuronal nitric oxide, *Nat. Cell Biol.* 3 (2) (2001) 193–197.
- [40] P.T. Doulias, K. Raju, J.L. Greene, M. Tenopoulou, H. Ischiropoulos, Mass

- spectrometry-based identification of S-nitrosocysteine in vivo using organic mercury assisted enrichment, *Methods* 62 (2) (2013) 165–170.
- [41] M. Yang, L. Luna, J.G. Sorbo, I. Alseth, R.F. Johansen, P.H. Backe, N.C. Danbolt, L. Eide, M. Bjoras, Human OXRL1 maintains mitochondrial DNA integrity and counteracts hydrogen peroxide-induced oxidative stress by regulating antioxidant pathways involving p21, *Free Radic. Biol. Med.* 77 (2014) 41–48.
 - [42] J. Goemaere, B. Knoop, Peroxiredoxin distribution in the mouse brain with emphasis on neuronal populations affected in neurodegenerative disorders, *J. Comp. Neurol.* 520 (2) (2012) 258–280.
 - [43] F. Hattori, S. Oikawa, Peroxiredoxins in the central nervous system, *Subcell. Biochem.* 44 (2007) 357–374.
 - [44] T.A. Sarafian, M.A. Verity, H.V. Vinters, C.C. Shih, L. Shi, X.D. Ji, L. Dong, H. Shau, Differential expression of peroxiredoxin subtypes in human brain cell types, *J. Neurosci. Res.* 56 (2) (1999) 206–212.
 - [45] E.S. Lein, M.J. Hawrylycz, N. Ao, M. Ayres, A. Bensinger, A. Bernard, A.F. Boe, M.S. Boguski, K.S. Brockway, E.J. Byrnes, L. Chen, L. Chen, T.M. Chen, M.C. Chin, J. Chong, B.E. Crook, A. Czaplinska, C.N. Dang, S. Datta, N.R. Dee, A.L. Desaki, T. Desta, E. Diep, T.A. Dolbeare, M.J. Donelan, H.W. Dong, J.G. Dougherty, B.J. Duncan, A.J. Ebbert, G. Eichele, L.K. Estlin, C. Faber, B.A. Facer, R. Fields, S.R. Fischer, T.P. Fliss, C. Frensley, S.N. Gates, K.J. Glattfelder, K.R. Halverson, M.R. Hart, J.G. Hohmann, M.P. Howell, D.P. Jeung, R.A. Johnson, P.T. Karr, R. Kaval, J.M. Kidney, R.H. Knapik, C.L. Kuan, J.H. Lake, A.R. Laramée, K.D. Larsen, C. Lau, T.A. Lemon, A.J. Liang, Y. Liu, L.T. Luong, J. Michaels, J.J. Morgan, R.J. Morgan, M.T. Mortrud, N.F. Mosqueda, L.L. Ng, R. Ng, G.J. Orta, C.C. Overly, T.H. Pak, S.E. Parry, S.D. Pathak, O.C. Pearson, R.B. Puchalski, Z.L. Riley, H.R. Rockett, S.A. Rowland, J.J. Royall, M.J. Ruiz, N.R. Sarno, K. Schaffnit, N.V. Shapovalova, T. Sivasay, C.R. Slaughterbeck, S.C. Smith, K.A. Smith, B.I. Smith, A.J. Sodt, N.N. Stewart, K.R. Stumpf, S.M. Sunkin, M. Sutram, A. Tam, C.D. Teemer, C. Thaller, C.L. Thompson, L.R. Varnam, A. Visel, R.M. Whitlock, P.E. Wohnoutka, C.K. Wolkey, V.Y. Wong, M. Wood, M.B. Yaylaoğlu, R.C. Young, B.L. Youngstrom, X.F. Yuan, B. Zhang, T.A. Zwingman, A.R. Jones, Genome-wide atlas of gene expression in the adult mouse brain, *Nature* 445 (7124) (2007) 168–176.
 - [46] S.U. Kim, M.H. Jin, Y.S. Kim, S.H. Lee, Y.S. Cho, K.J. Cho, K.S. Lee, Y.I. Kim, G.W. Kim, J.M. Kim, T.H. Lee, Y.H. Lee, M. Shong, H.C. Kim, K.T. Chang, D.Y. Yu, D.S. Lee, Peroxiredoxin II preserves cognitive function against age-linked hippocampal oxidative damage, *Neurobiol. Aging* 32 (6) (2011) 1054–1068.
 - [47] H.H. Jang, K.O. Lee, Y.H. Chi, B.G. Jung, S.K. Park, J.H. Park, J.R. Lee, S.S. Lee, J.C. Moon, J.W. Yun, Y.O. Choi, W.Y. Kim, J.S. Kang, G.W. Cheong, D.J. Yun, S.G. Rhee, M.J. Cho, S.Y. Lee, Two enzymes in one; two yeast peroxiredoxins display oxidative stress-dependent switching from a peroxidase to a molecular chaperone function, *Cell* 117 (5) (2004) 625–635.
 - [48] J.C. Moon, Y.S. Hah, W.Y. Kim, B.G. Jung, H.H. Jang, J.R. Lee, S.Y. Kim, Y.M. Lee, M.G. Jeon, C.W. Kim, M.J. Cho, S.Y. Lee, Oxidative stress-dependent structural and functional switching of a human 2-Cys peroxiredoxin isotype II that enhances HeLa cell resistance to H₂O₂-induced cell death, *J. Biol. Chem.* 280 (31) (2005) 28775–28784.
 - [49] H.H. Jang, S.Y. Kim, S.K. Park, H.S. Jeon, Y.M. Lee, J.H. Jung, S.Y. Lee, H.B. Chae, Y.J. Jung, K.O. Lee, C.O. Lim, W.S. Chung, J.D. Bahk, D.J. Yun, M.J. Cho, S.Y. Lee, Phosphorylation and concomitant structural changes in human 2-Cys peroxiredoxin isotype I differentially regulate its peroxidase and molecular chaperone functions, *FEBS Lett.* 580 (1) (2006) 351–355.
 - [50] T.J. Phalen, K. Weirather, P.B. Deming, V. Anathy, A.K. Howe, A. van der Vliet, T.J. Jonsson, L.B. Poole, N.H. Heintz, Oxidation state governs structural transitions in peroxiredoxin II that correlate with cell cycle arrest and recovery, *J. Cell Biol.* 175 (5) (2006) 779–789.
 - [51] E.A. Veal, Z.E. Underwood, L.E. Tomalin, B.A. Morgan, C.S. Pillay, Hyperoxidation of peroxiredoxins: gain or loss of function? *Antioxid. Redox Signal.* 28 (7) (2018) 574–590.
 - [52] Y. Gan, X. Ji, X. Hu, Y. Luo, L. Zhang, P. Li, X. Liu, F. Yan, P. Vosler, Y. Gao, R.A. Stetler, J. Chen, Transgenic overexpression of peroxiredoxin-2 attenuates ischemic neuronal injury via suppression of a redox-sensitive pro-death signaling pathway, *Antioxid. Redox Signal.* 17 (5) (2012) 719–732.
 - [53] S. Zhou, Q. Han, R. Wang, X. Li, Q. Wang, H. Wang, J. Wang, Y. Ma, PRDX2 protects hepatocellular carcinoma SMMC-7721 cells from oxidative stress, *Oncol. Lett.* 12 (3) (2016) 2217–2221.
 - [54] B. Manta, M. Hugo, C. Ortiz, G. Ferrer-Sueta, M. Trujillo, A. Denicola, The peroxidase and peroxynitrite reductase activity of human erythrocyte peroxiredoxin 2, *Arch. Biochem. Biophys.* 484 (2) (2009) 146–154.
 - [55] A.V. Peskin, N. Dickerhof, R.A. Poynton, L.N. Paton, P.E. Pace, M.B. Hampton, C.C. Winterbourn, Hyperoxidation of peroxiredoxins 2 and 3: rate constants for the reactions of the sulfenic acid of the peroxidic cysteine, *J. Biol. Chem.* 288 (20) (2013) 14170–14177.
 - [56] E.M. Lee, S.S. Lee, B.N. Tripathi, H.S. Jung, G.P. Cao, Y. Lee, S. Singh, S.H. Hong, K.W. Lee, S.Y. Lee, J.Y. Cho, B.Y. Chung, Site-directed mutagenesis substituting cysteine for serine in 2-Cys peroxiredoxin (2-Cys Prx A) of *Arabidopsis thaliana* effectively improves its peroxidase and chaperone functions, *Ann. Bot.* 116 (4) (2015) 713–725.
 - [57] Z.T. Farahbakhsh, Q.L. Huang, L.L. Ding, C. Altenbach, H.J. Steinhoff, J. Horwitz, W.L. Hubbell, Interaction of alpha-crystallin with spin-labeled peptides, *Biochemistry* 34 (2) (1995) 509–516.
 - [58] J. Fang, T. Nakamura, D.H. Cho, Z. Gu, S.A. Lipton, S-nitrosylation of peroxiredoxin 2 promotes oxidative stress-induced neuronal cell death in Parkinson's disease, *Proc. Natl. Acad. Sci. USA* 104 (47) (2007) 18742–18747.
 - [59] Y. Ogasawara, T. Ohminato, Y. Nakamura, K. Ishii, Structural and functional analysis of native peroxiredoxin 2 in human red blood cells, *Int. J. Biochem. Cell Biol.* 44 (7) (2012) 1072–1077.
 - [60] A.V. Peskin, P.E. Pace, J.B. Behring, L.N. Paton, M. Soethoudt, M.M. Bachschmid, C.C. Winterbourn, Glutathionylation of the active site cysteines of peroxiredoxin 2 and recycling by glutaredoxin, *J. Biol. Chem.* 291 (6) (2016) 3053–3062.
 - [61] P.A. Karplus, A primer on peroxiredoxin biochemistry, *Free Radic. Biol. Med.* 80 (2015) 183–190.
 - [62] M.M. Stacey, M.C. Viessers, C.C. Winterbourn, Oxidation of 2-cys peroxiredoxins in human endothelial cells by hydrogen peroxide, hypochlorous acid, and chloramines, *Antioxid. Redox Signal.* 17 (3) (2012) 411–421.
 - [63] S.R. Jaffrey, S.H. Snyder, The biotin switch method for the detection of S-nitrosylated proteins, *Sci. STKE* 2001 (86) (2001) 11.
 - [64] H.Z. Chae, H.J. Kim, S.W. Kang, S.G. Rhee, Characterization of three isoforms of mammalian peroxiredoxin that reduce peroxides in the presence of thioredoxin, *Diabetes Res. Clin. Pract.* 45 (2–3) (1999) 101–112.
 - [65] C.R. Sunico, A. Sultan, T. Nakamura, N. Dolatabadi, J. Parker, B. Shan, X. Han, J.R. Yates 3rd, E. Masliah, R. Ambasudhan, N. Nakanishi, S.A. Lipton, Role of sulfiredoxin as a peroxiredoxin-2 denitrosylase in human iPSC-derived dopaminergic neurons, *Proc. Natl. Acad. Sci. USA* 113 (47) (2016) E7564–E7571.
 - [66] D. Qu, J. Rashidian, M.P. Mount, H. Aleyasin, M. Parsanejad, A. Lira, E. Haque, Y. Zhang, S. Callaghan, M. Daigle, M.W. Rousseaux, R.S. Slack, P.R. Albert, I. Vincent, J.M. Woulfe, D.S. Park, Role of Cdk5-mediated phosphorylation of Prx2 in MPTP toxicity and Parkinson's disease, *Neuron* 55 (1) (2007) 37–52.